SCIENCE CHINA
Mathematics

Progress of Projects Supported by NSFC
• ARTICLES •

December 2013 Vol. 56 No. 12: 2571–2589
doi: 10.1007/s11425-013-4726-6

The effect of ghost forces for a quasicontinuum method in three dimension

Dedicated to Professor Shi Zhong-Ci on the Occasion of his 80th Birthday

CUI Long & MING PingBing*

LSEC, Institute of Computational Mathematics and Scientific/Engineering Computing, Academy of Mathematics and Systems Science, Chinese Academy of Sciences, Beijing 100190, China
Email: cuilong@lsec.cc.ac.cn, mpb@lsec.cc.ac.cn

Received May 2, 2013; accepted July 26, 2013; published online October 16, 2013

Abstract We study the effect of "ghost forces" for a quasicontinuum method in three dimension with a planar interface. "Ghost forces" are the inconsistency of the quasicontinuum method across the interface between the atomistic region and the continuum region. Numerical results suggest that "ghost forces" may lead to a negilible error on the solution, while lead to a finite size error on the gradient of the solution. The error has a layer-like profile, and the interfacial layer width is of $O(\varepsilon)$. The error in certain component of the displacement gradient decays algebraically from $O(1)$ to $O(\varepsilon)$ away from the interface. A surrogate model is proposed and analyzed, which suggests the same scenario for the effect of "ghost forces". Our analysis is based on the explicit solution of the surrogate model.

Keywords quasicontinuum method, atomistic-to-continuum, ghost force

MSC(2010) 65N30, 65N12, 65N06, 74G20, 74G15

Citation: Cui L, Ming P B. The effect of ghost forces for a quasicontinuum method in three dimension. Sci China Math, 2013, 56: 2571–2589, doi: 10.1007/s11425-013-4726-6

1 Introduction

Multiscale methods that couple the atomistic model and the continuum model have been extensively studied over the past few decades, and these methods have been employed to simulate various properties of materials, in particular for solids [1, 5, 14]. One critical issue of these methods is the so-called *ghost force*, which is the none-zero force that atoms experience at the undeformed state [19]. From the numerical analysis aspect of view, ghost force is nothing but the inconsistency of the method. Some efforts have been devoted to studying the effect of the ghost force. The ghost force issue for the one-dimensional problem is well-understood now, see [4, 15, 16]. The main findings are nicely summarized in [5, p. 278]: (1) the ghost force induces a negligible error on the solution, which is usually as small as the lattice spacing, while it may lead to an $\mathcal{O}(1)$ error on the gradient of the solution; (2) the influence of the ghost force decays exponentially fast away from the interface; (3) away from the interfacial layer of width $\mathcal{O}(\varepsilon|\ln\varepsilon|)$, the error in the displacement gradient is of $\mathcal{O}(\varepsilon)$ with ε being the lattice spacing. The effect of the ghost force for a two-dimensional problem with a planar atomistic to continuum (a/c) interface has recently been carried out in [3]. The story is almost the same except that the decay of the error in the displacement gradient is much slower than that of the one-dimensional problem. The decay rate is algebraical, and

*Corresponding author

away from the interfacial layer of width at most $\mathcal{O}(\sqrt{\varepsilon})$, the error in the displacement gradient is of $\mathcal{O}(\varepsilon)$. Identifying the effect of the ghost force for the dynamical problem is largely unexplored, but we refer to [11] for a preliminary study.

For statics problems, the elimination of the ghost force is a necessary ingredient to achieve uniform accuracy [6, 17]. It is worth mentioning some work on the convergence analysis for the ghost force free multiscale coupling methods in high dimension, we refer to [12, 13, 18] for the related work.

The aim of this work is to quantify the error caused by the ghost force for a quasicontinuum method (QC) [7, 20] in three dimensions. QC is a representative multiscale coupling method. We begin by studying a face-centered cubic (FCC) lattice model interacted with Lennard-Jones potential [10]. The Cauchy-Born (CB) elasticity model [2] couples with the atomistic model. Numerical results suggest that the displacement gradient has an $\mathcal{O}(1)$ error as those of one and two-dimensional problems. The error has a layer-like profile and the layer width is of $\mathcal{O}(\varepsilon)$. Moreover, the displacement gradient decays from $\mathcal{O}(1)$ to $\mathcal{O}(\varepsilon)$ algebraically away from the interface.

To understand such phenomenon, we propose a cubic lattice model with a special interaction range and a QC approximation, which is in the same spirit of the one studied in [3]. Numerical results give the same scenario as those of the FCC lattice model with a QC approximation. This model admits an analytical solution, which is exploited to prove that the displacement gradient indeed decays algebraically away from the interface.

The paper is organized as follows. Numerical results for the FCC lattice model with a QC approximation and the cubic lattice model with a QC approximation are presented in Sections 2 and 3, respectively. In Section 4, we derive an analytical solution to the cubic lattice model, and the pointwise estimates of the error are obtained in Section 5. We draw the conclusion in the last section. Some detailed derivation omitted in Section 3 can be found in Appendixes A and B.

2 A QC method for FCC lattice

2.1 Atomistic and continuum models for FCC lattice

We consider the FCC lattice $\mathbb{L}$, which can be written as

$$\mathbb{L} = \{\, x \in \mathbb{R}^3 \mid x = ps_1 + qs_2 + rs_3, p, q, r \in \mathbb{Z} \,\}$$

with the basis vectors $s_1 = (1/2, 1/2, 0)$, $s_2 = (0, 1/2, 1/2)$ and $s_3 = (1/2, 0, 1/2)$. The domain Ω is defined as $\Omega = \{\, x = x_1 s_1 + x_2 s_2 + x_3 s_3 \mid 0 \leqslant x_1, x_2 < 1/2, -1/2 \leqslant x_3 < 1/2 \,\}$. Let $\Omega_\varepsilon = \Omega \cap \varepsilon\mathbb{L}$ with $\varepsilon = 1/(2N)$ being the equilibrium bond length. If the third nearest neighbor interaction is considered, then the total energy of the system is

$$E_{\mathrm{at}}^{\mathrm{tot}}[y](x) = \frac{1}{2} \sum_{x \in \Omega_\varepsilon} \sum_{x' \in x + \mathcal{S}} V(|y(x) - y(x')|),$$

where V is the Lennard-Jones potential and the interaction range $\mathcal{S} = S_1 \cup S_2 \cup S_3$ with

$$\begin{aligned} S_1 &= \{\pm s_1, \pm s_2, \pm s_3, \pm(s_1 - s_2), \pm(s_1 - s_3), \pm(s_2 - s_3)\}, \\ S_2 &= \{\pm(s_2 + s_3 - s_1), \pm(s_1 + s_2 - s_3), \pm(s_1 + s_3 - s_2)\}, \end{aligned}$$

and

$$\begin{aligned} S_3 = \{&\pm(2s_1 - s_2), \pm(s_1 + s_2), \pm(2s_2 - s_1), \pm(2s_2 - s_3), \pm(s_1 + s_2), \\ &\pm(2s_3 - s_1), \pm(2s_1 - s_2), \pm(s_1 + s_2), \pm(2s_3 - s_2), \pm(2s_1 - s_1 - s_2), \\ &\pm(2s_2 - s_1 - s_3), \pm(2s_3 - s_1 - s_2)\}. \end{aligned}$$

Let $\Omega_c = \{\, x \in \Omega \mid x_3 > 0 \,\}$ and $\Omega_a = \Omega_\varepsilon \setminus \overline{\Omega}_c$. In Ω_a, we use the atomistic model, and in Ω_c we use the continuum model with the stored energy functional

$$E_{\Omega_c}^{\mathrm{CB}} = \int_{\Omega_c} W_{\mathrm{CB}}(\nabla y(x)) dx$$

with $W_{\rm CB}(\nabla y) = \frac{1}{2\vartheta_0}\sum_{s\in\mathcal{S}} V(|(s\cdot\nabla)y|)$, where $y(x)$ is the deformation of x-th atom, and ϑ_0 is the volume of the unit cell of $\mathbb{L}$. Since we are primarily interested in the coupling between the atomistic and continuum models, we will take the finite element mesh as a triangulation of Ω_ε with each atom site as an element vertex. The linear finite element is used to approximate $W_{\rm CB}$. The total energy of the coupled system is given by

$$E^{\rm tot}[y](x) = \frac{1}{2}\sum_{x\in\Omega_a}\sum_{x'\in x+\mathcal{S}} V(|y(x')-y(x)|) + \frac{1}{2}\sum_{x_3=0}\sum_{\substack{x'\in x+\mathcal{S}\\ x_3'\leqslant 0}} V(|y(x)-y(x')|) + E^{\rm CB}_{\Omega_c,\varepsilon},$$

where $E^{\rm CB}_{\Omega_c,\varepsilon}$ is the finite element approximation of $E^{\rm CB}_{\Omega_c}$. We minimize $E^{\rm tot}$ with respect to $y(x)$ subject to the Dirichlet boundary condition $y(x)=x$ for $x\in\partial\Omega_\varepsilon$, where the boundary $\partial\Omega_\varepsilon$ is defined as

$$\partial\Omega_\varepsilon = \partial\Omega_\varepsilon^1\cup\partial\Omega_\varepsilon^2\cup\partial\Omega_\varepsilon^3$$

with

$$\begin{aligned}
\partial\Omega_\varepsilon^1 &= \{\, x\in\varepsilon\mathbb{L} \mid p\in\{-2,-1,N+1,N+2\}, q=0,\dots,N, r=-N,\dots,N\,\},\\
\partial\Omega_\varepsilon^2 &= \{\, x\in\varepsilon\mathbb{L} \mid q\in\{-2,-1,N+1,N+2\}, p=0,\dots,N, r=-N,\dots,N\,\},\\
\partial\Omega_\varepsilon^3 &= \{\, x\in\varepsilon\mathbb{L} \mid r\in\{-N-2,-N-1,N+1,N+2\}, p,q=0,\dots,N\,\}.
\end{aligned}$$

The Euler-Lagrangian equation of the above minimization problem is

$$\mathcal{L}_{\rm qc}[y(x)] = 0, \tag{2.1}$$

where $\mathcal{L}_{\rm qc}$ is the variational operator of $E^{\rm tot}$. The displacement $u(x) := y(x) - x$ satisfies

$$\mathcal{L}_{\rm qc}[u(x)+x] = 0.$$

If $\mathcal{L}_{\rm qc}$ is linear, then

$$\mathcal{L}_{\rm qc}[u(x)] = f(x) \quad \text{with} \quad f(x) := -\mathcal{L}_{\rm qc}[x]. \tag{2.2}$$

The source term $f(x)$ is the so-called ghost force. The effect of the ghost force is characterized by $u(x)$.

2.2 Numerical results

We solve (2.1) and find that all components of u have a clear layer-like profile. For brevity we only plot u_3 and its discrete gradient D_iu_3 in Figure 1, where

$$D_iu(x) := (u(x+\varepsilon s_i)-u(x))/\varepsilon, \quad i=1,2,3.$$

Motivated by the previous study in [3, 4, 16], the maximum of Du is the main quantity of interest, and we report $\|Du\|_\infty := \max_{i,j=1}^3 \|D_iu_j\|_{L^\infty(\Omega_\varepsilon)}$ in Table 1. The result suggests that Du is uniformly bounded with respect to ε. In view of Figure 1, we find that D_3u_3 also has a layer-like profile. It would be interesting to find the layer width and the decay rate of D_3u_3. The definition of the layer width is slightly different from that of [3]. It reads as

$$d := \max_{p,q}(\overline{r}-\underline{r})(p,q)\varepsilon,$$

where

$$\begin{aligned}
\overline{r}(p,q) &= \operatorname*{argmin}_{r>r^*(p,q)} \quad \text{such that} \quad |D_3u_3(p,q,r)| \leqslant \frac{1}{2}|D_3u_3(p,q,r^*)|,\\
\underline{r}(p,q) &= \operatorname*{argmax}_{r<r^*(p,q)} \quad \text{such that} \quad |D_3u_3(p,q,r)| \leqslant \frac{1}{2}|D_3u_3(p,q,r^*)|,
\end{aligned}$$

and

$$r^*(p,q) = \operatorname*{argmax}_r |D_3u_3(p,q,r)|.$$

Table 2 shows that the width of the interfacial layer is of $\mathcal{O}(\varepsilon)$.

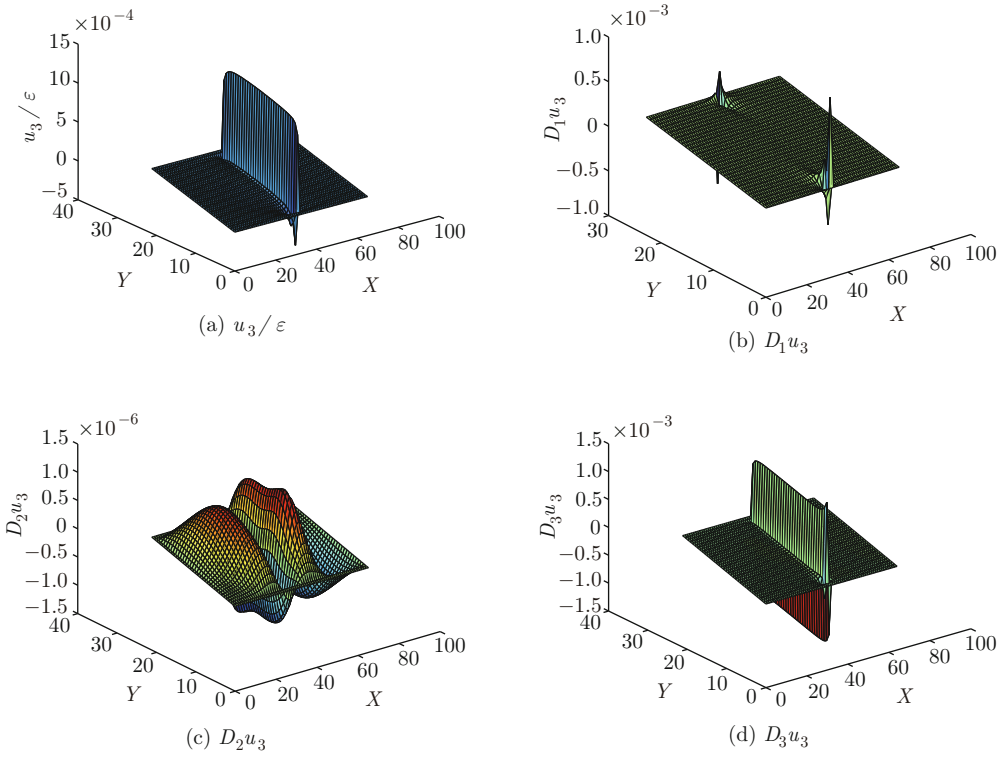

Figure 1 The sectional view of $u_3(p,q,r)$ and its discrete gradient when $N=31$ and $q=18$

Table 1 $\|Du\|_\infty$ versus the equilibrium bond length ε

ε	2^{-4}	2^{-5}	2^{-6}	2^{-7}	2^{-8}
$\|Du\|_\infty$	1.674e−3	1.675e−3	1.675e−3	1.675e−3	1.675e−3

Table 2 The layer width d versus the equilibrium bond length ε

ε	2^{-4}	2^{-5}	2^{-6}	2^{-7}	2^{-8}
d	1.28e−1	6.4e−2	3.2e−2	1.6e−2	8e−3

To get the decay rate of D_3u_3, we need a threshold value c_0. For fixed p and q, we find two points $(p,q,\underline{r})$ and $(p,q,\overline{r})$ with $\overline{r}$ and $\underline{r}$ defined by

$$\overline{r}(p,q)=\operatorname*{argmax}_r \quad \text{such that} \quad |D_3u_3|(p,q,r)>c_0\varepsilon,$$
$$\underline{r}(p,q)=\operatorname*{argmin}_r \quad \text{such that} \quad |D_3u_3|(p,q,r)>c_0\varepsilon.$$

The decay rate R is defined by

$$R:=\log\max_{p,q}(\overline{r}-\underline{r})(p,q)\varepsilon/\log\varepsilon.$$

We report the decay rate in Table 3 for different c_0. The decay rate seems to be close to 1/2. Though we cannot prove this fact, we shall give an explanation on this observation by using the lattice Green's function in the end of Section 5.

Since the operator $\mathcal{L}_{\rm qc}$ coincides with $\mathcal{L}_{\rm cb}$ in the local region, where $\mathcal{L}_{\rm cb}$ is the variational operator associated with $W_{\rm CB}$, it is natural to look at a similar model to (2.1), where $\mathcal{L}_{\rm qc}$ is replaced by $\mathcal{L}_{\rm cb}$. We replace $\mathcal{L}_{\rm qc}$ by $\mathcal{L}_{\rm cb}$ in the left-hand side of (2.2) and obtain

$$\mathcal{L}_{\rm cb}[u(x)+x]=-\mathcal{L}_{\rm qc}[x]. \tag{2.3}$$

Table 3 The decay rate R with respect to different c_0 versus the equilibrium bond length ε

ε	2^{-4}	2^{-5}	2^{-6}	2^{-7}	2^{-8}	rate (R)
$c_0 = 0.0004$	0.500	0.366	0.264	0.192	0.137	0.467
$c_0 = 0.0008$	0.357	0.254	0.188	0.134	0.097	0.468
$c_0 = 0.0012$	0.288	0.210	0.143	0.109	0.079	0.469
$c_0 = 0.0016$	0.270	0.186	0.129	0.095	0.068	0.496

The profiles for u_3 and D_3u_3 can be found in Figure 2, and we report $\|Du\|_\infty$ in Table 4, which shows that Du is uniformly bounded with respect to ε. By Table 5, we conclude that the layer width is of $\mathcal{O}(\varepsilon)$. Choosing different c_0, we report the decay rate in Table 6. It is clear that the decay rate is still close to 1/2. These evidences show that the model (2.3) may be viewed as a *surrogate* model for the original FCC lattice model.

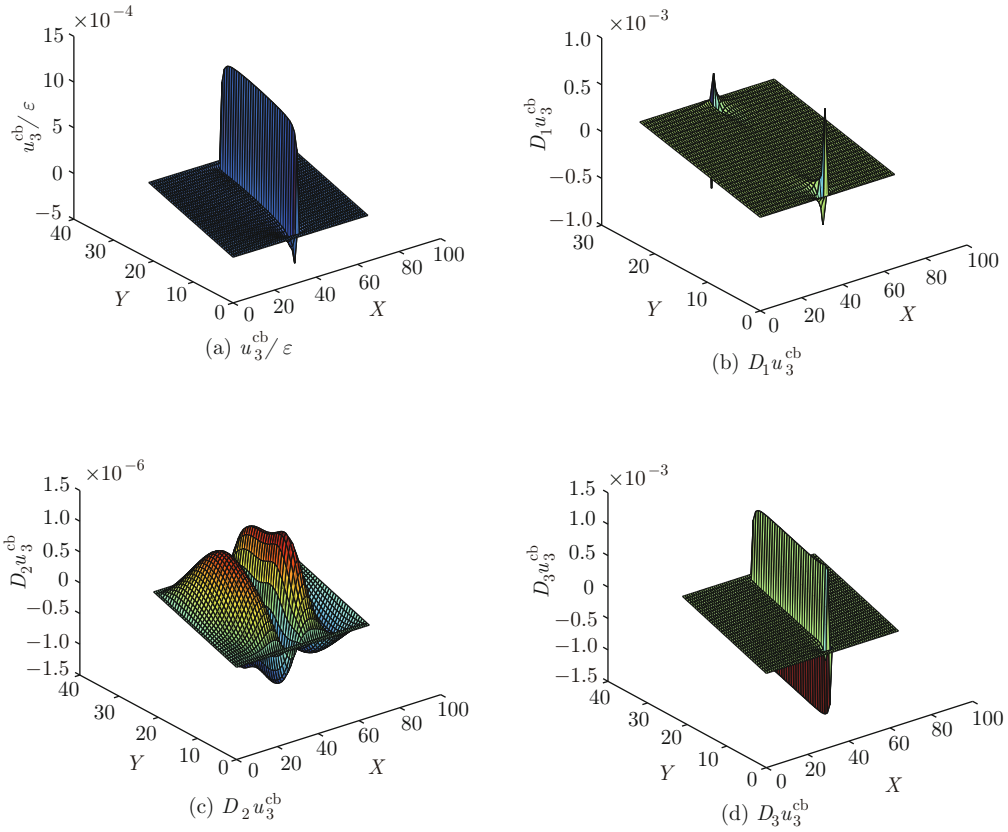

Figure 2 The sectional view of $u_3(p,q,r)^{\rm cb}$ and its gradient when $N = 31$ and $q = 18$

Table 4 $\|Du\|_\infty$ versus the equilibrium bond length ε

ε	2^{-4}	2^{-5}	2^{-6}	2^{-7}	2^{-8}
$\|Du\|_\infty$	1.545e−3	1.546e−3	1.546e−3	1.546e−3	1.546e−3

Table 5 The layer width d versus the equilibrium bond length ε

ε	2^{-4}	2^{-5}	2^{-6}	2^{-7}	2^{-8}
d	1.28e−1	6.4e−2	3.2e−2	1.6e−2	8.0e−3

Table 6 The decay rate R with respect to different c_0 versus the equilibrium bond length ε

ε	2^{-4}	2^{-5}	2^{-6}	2^{-7}	2^{-8}	rate (R)
$c_0 = 0.0004$	0.496	0.365	0.265	0.192	0.136	0.467
$c_0 = 0.0008$	0.334	0.250	0.184	0.135	0.095	0.451
$c_0 = 0.0012$	0.281	0.200	0.142	0.109	0.078	0.459
$c_0 = 0.0016$	0.254	0.171	0.126	0.094	0.067	0.473

3 A QC method for cubic lattice

In this section, we introduce a cubic lattice model that is motivated by the square lattice model proposed in [3]. We shall show in the next two sections that this model not only captures the main features of the FCC lattice model described in the last section, but also lends itself theoretically tractable, i.e., this model can be solved *exactly*. Therefore, it may be viewed as a suitable *surrogate* model for the original FCC lattice model.

3.1 Setup and formulation

We consider a simple cubic lattice $\mathbb{L}$ interacted with the harmonic potential. The domain $\Omega := (0,1) \times (-1,1) \times (0,1)$, and we denote $\Omega_\varepsilon = \Omega \cap \varepsilon\mathbb{L}$ with $\varepsilon = 1/N$. We assume the nearest neighbor interaction for x-direction and z-direction, and next-to-nearest neighbor interaction in y-direction. The neighbors of a point p_0 are shown in Figure 3(a).

For any lattice function $u : \Omega_\varepsilon \to \mathbb{R}^3$, we let $u(p,q,r) = u(x)$ with $x = (p,q,r)\varepsilon$, where the labels $p, r = 0, \ldots, N$ and $q = -N, \ldots, N$. We employ the atomistic model for the region with $|x_2| \leqslant K\varepsilon$, and outside this region, the CB elastic model is used. The domain Ω is illustrated in Figure 3(b). We assume that the total energy $E = \sum_{x\in\Omega_\varepsilon} E_x$ with

$$E_x = \frac{\kappa_1}{2} \sum_{|x'-x|=\varepsilon} |y(x') - y(x)|^2 + \frac{\kappa_2}{2}(|y(x_1, x_2 - 2\varepsilon, x_3) - y(x)|^2 + |y(x_1, x_2 + 2\varepsilon, x_3) - y(x)|^2),$$

where $|x' - x| := |x'_1 - x_1| + |x'_2 - x_2| + |x'_3 - x_3|$, and κ_1 and κ_2 are the force constants computed from the interatomic potential. We assume that $\kappa_2 < 0$.

For $|x_2| \leqslant (K-2)\varepsilon$, $\mathcal{L}_{\rm qc}[u(x)] = \mathcal{L}_{\rm at}[u(x)]$ with

$$\mathcal{L}_{\rm at}[u(x)] := 2(3\kappa_1 + \kappa_2)u(x) - \kappa_1 \sum_{|x'-x|=\varepsilon} u(x') - \kappa_2(u(x_1, x_2 + 2\varepsilon, x_3) + u(x_1, x_2 - 2\varepsilon, x_3)).$$

For $|x_2| \geqslant (K+2)\varepsilon$, $\mathcal{L}_{\rm qc}[u](x) = \mathcal{L}_{\rm cb}[u](x)$ with

$$\begin{aligned}\mathcal{L}_{\rm cb}[u(x)] := {} & 2(3\kappa_1 + 4\kappa_2)u(x) - \kappa_1(u(x_1 - \varepsilon, x_2, x_3) + u(x_1 + \varepsilon, x_2, x_3)) \\ & - (\kappa_1 + 4\kappa_2)(u(x_1, x_2 - \varepsilon, x_3) + u(x_1, x_2 + \varepsilon, x_3)) \\ & - \kappa_1(u(x_1, x_2, x_3 - \varepsilon) + u(x_1, x_2, x_3 + \varepsilon)).\end{aligned}$$

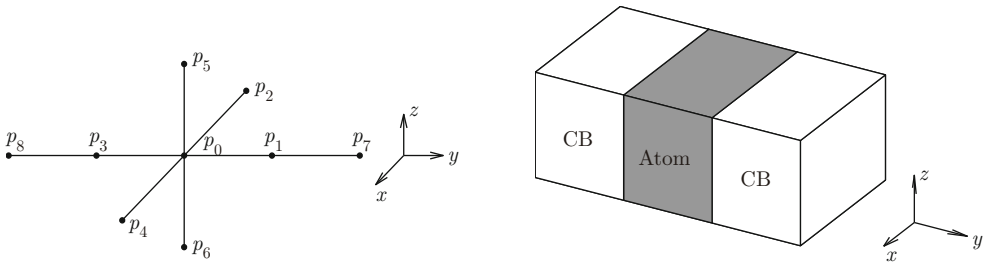

(a) The interaction range for atom p_0 (b) The CB-Atom-CB coupling model

Figure 3 Interaction range and the domain Ω

In the interfacial region, when $x_2 = (K-1)\varepsilon$,

$$\mathcal{L}_{\rm qc}[u(x)] := (6\kappa_1 + 3\kappa_2/2)\,u(x) - \kappa_1 \sum_{|x'-x|=\varepsilon} u(x') - \frac{\kappa_2}{2}u(x_1, x_2+2\varepsilon, x_3) - \kappa_2 u(x_1, x_2-2\varepsilon, x_3).$$

When $x_2 = -(K-1)\varepsilon$, we obtain the expression of $\mathcal{L}_{\rm qc}$ by replacing the second coordinate of $u(x)$ by its inversion, i.e., $u(x_1, x_2, x_3)$ is replaced by $u(x_1, -x_2, x_3)$. This rule applies to the other interfacial equations.

When $x_2 = K\varepsilon$,

$$\mathcal{L}_{\rm qc}[u(x)] := (6\kappa_1 + 5\kappa_2)\,u(x) - \kappa_1 \sum_{\substack{|x'-x|=\varepsilon,\\ x_2'\neq(K+1)\varepsilon}} u(x') - (\kappa_1+4\kappa_2)u(x_1, x_2+\varepsilon, x_3) - \kappa_2 u(x_1, x_2-2\varepsilon, x_3).$$

When $x_2 = (K+1)\varepsilon$,

$$\begin{aligned}\mathcal{L}_{\rm qc}[u(x)] := (6\kappa_1 + 17\kappa_2/2)\,u(x) - \kappa_1 &\sum_{\substack{|x'-x|=\varepsilon,\\ x_2'\neq(K+2)\varepsilon, x_2'\neq K\varepsilon}} u(x') \\ &- (\kappa_1+4\kappa_2)(u(x_1, x_2+\varepsilon, x_3) + u(x_1, x_2-\varepsilon, x_3)) - \frac{\kappa_2}{2}u(x_1, x_2-2\varepsilon, x_3).\end{aligned}$$

It is clear that for all $x \in \Omega_\varepsilon$, we have $\mathcal{L}_{\rm qc}[x]_1 = \mathcal{L}_{\rm qc}[x]_3 = 0$, and

$$\mathcal{L}_{\rm qc}[x]_2 = \begin{cases} 0, & x_2 \geqslant (K+2)\varepsilon \quad \text{or} \quad x_2 \leqslant (2-K)\varepsilon, \\ \kappa_2\varepsilon\,\mathrm{sgn}(x_2), & |x_2| = (K-1)\varepsilon, \\ -2\kappa_2\varepsilon\,\mathrm{sgn}(x_2), & |x_2| = K\varepsilon, \\ \kappa_2\varepsilon\,\mathrm{sgn}(x_2), & |x_2| = (K+1)\varepsilon. \end{cases}$$

In what follows, we only study the second component of $u(x)$, which is also denoted by $u(x)$. It satisfies

$$\mathcal{L}_{\rm qc}[u(x)] = f(x) \tag{3.1}$$

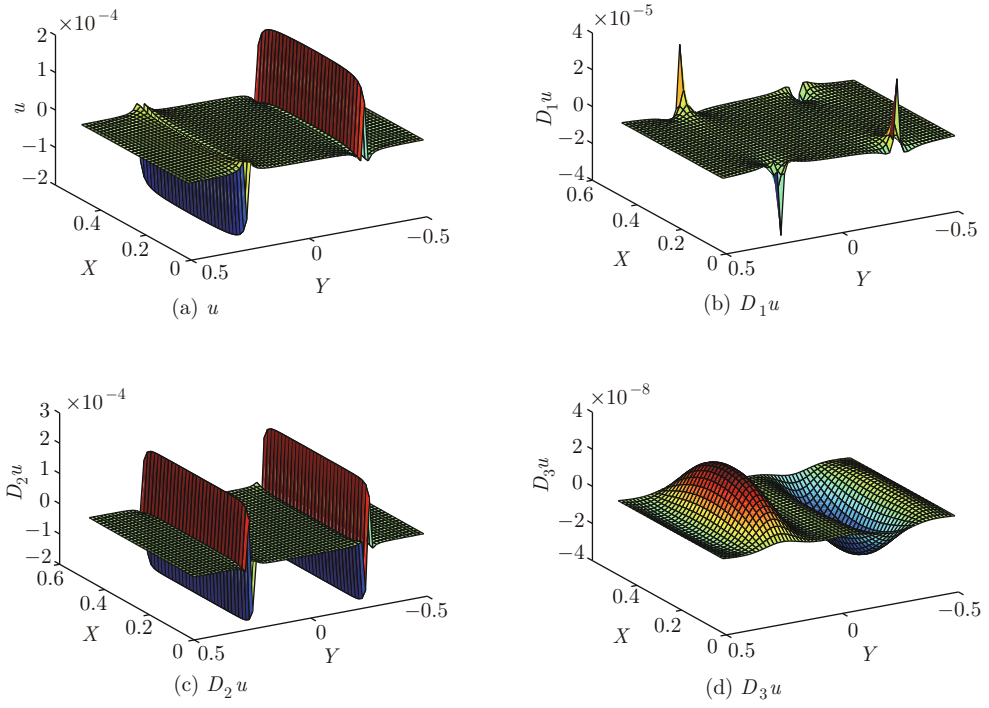

Figure 4 The XOY sectional view of u and its gradients when $N = 31$, $z = 0.25$ and $K = (N+1)/2$

with $f(x) = -\mathcal{L}_{\rm qc}[x]$. We supplement the above equation with the Dirichlet boundary condition $u(x) = 0$ for $x \in \partial\Omega_\varepsilon$.

By the symmetry of the domain Ω_ε and the operator $\mathcal{L}_{\rm qc}$, we conclude that the solution is odd in y-direction. Therefore, we only consider the domain with $x_2 \geqslant 0$, i.e., Ω is a unit cube $(0,1)^3$. In this case, the term $\mathrm{sgn}(x_2)$ in $f(x)$ vanishes.

3.2 Numerical results

Let $\kappa_1 = 60.093$ and $\kappa_2 = -0.741379$ in (3.1). The profiles for u and Du can be found in Figures 4 and 5 when $N = 31$ with different positions of the a/c interface.

We report $\|Du\|_\infty$ in Table 7 for different positions of the a/c interface K and the lattice spacing ε.

Table 8 shows that the layer width is of $\mathcal{O}(\varepsilon)$.

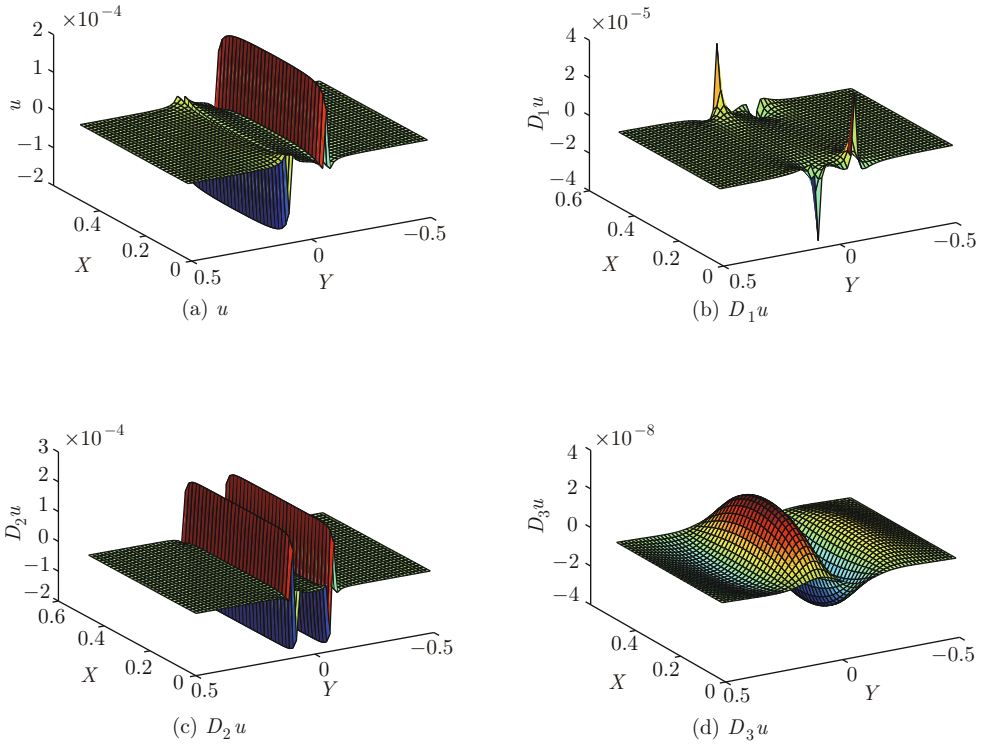

Figure 5 The XOY sectional view of $u(\cdot, 0.25)$ and its gradients when $N = 31$ and $K = \sqrt{N+1}$

Table 7 $\|Du\|_\infty$ versus the equilibrium bond length ε for different positions of the a/c interface

ε	2^{-5}	2^{-6}	2^{-7}	2^{-8}	2^{-9}
$\|Du\|_\infty$ $(K = (N+1)/2)$	1.292e−2	1.296e−2	1.297e−2	1.298e−2	1.298e−2
$\|Du\|_\infty$ $(K = \sqrt{N+1})$	1.298e−2	1.298e−2	1.298e−2	1.298e−2	1.298e−2

Table 8 The layer width d versus the equilibrium bond length ε

ε	2^{-5}	2^{-6}	2^{-7}	2^{-8}	2^{-9}
d $(K = (N+1)/2)$	6.787e−2	3.393e−2	1.697e−2	8.48e−3	4.24e−3
d $(K = \sqrt{N+1})$	6.787e−2	3.393e−2	1.697e−2	8.48e−3	4.24e−3

4 Exact solution to cubic lattice model

4.1 Representation of the solution

Using the ansatz of *separation of variables*, we obtain the following representation of u.

Theorem 4.1. *For $q = K+1, \dots, N$ and $p, r = 1, \dots, N$,*

$$u(p,q,r) = \sum_{k,l=1}^{N} a_{k,l} \sinh[(N-q)\alpha_{k,l}] \sin\frac{pk\pi}{N} \sin\frac{rl\pi}{N}$$

with

$$\cosh\alpha_{k,l} = 1 + \frac{\kappa_1}{\overline{\kappa}}(\lambda_k + \lambda_l),$$

where $\overline{\kappa} = \kappa_1 + 4\kappa_2$ and $\lambda_k = 2\sin^2 k\pi/[2N]$.

For $q = 1, \dots, K$ and $p, r = 1, \dots, N$,

$$u(p,q,r) = \sum_{k,l=1}^{N} (b_{k,l} \sinh[q\beta_{k,l}] + c_{k,l} \sinh[q\delta_{k,l}]) \sin\frac{pk\pi}{N} \sin\frac{rl\pi}{N},$$

where $\beta_{k,l}$ and $\delta_{k,l}$ are given by

$$\begin{cases} \cosh\beta_{k,l} = \dfrac{-\kappa_1 + \sqrt{\overline{\kappa}^2 + 8\kappa_1\kappa_2(\lambda_k+\lambda_l)}}{4\kappa_2}, \\ \cosh\delta_{k,l} = \dfrac{-\kappa_1 - \sqrt{\overline{\kappa}^2 + 8\kappa_1\kappa_2(\lambda_k+\lambda_l)}}{4\kappa_2}. \end{cases} \tag{4.1}$$

Here and in what follows, we denote $u(p,q,r)$ by $u_{\rm at}$ for $q = 1, \dots, K$, and $u_{\rm cb}$ for $q = K+1, \dots, N$.

Note that $\cosh\beta_{k,l} = a_1/2$ and $\cosh\delta_{k,l} = a_2/2$, where a_1 and a_2 are two roots of the quadratic equation

$$\kappa_2 x^2 + \kappa_1 x - 2\kappa_1(\lambda_k + \lambda_l) - 2(\kappa_1 + 2\kappa_2) = 0. \tag{4.2}$$

By definition, we have

$$2\kappa_2 \cosh^2 x + \kappa_1 \cosh x = \kappa_1(\lambda_k + \lambda_l + 1) + 2\kappa_2, \quad x = \beta_{k,l}, \delta_{k,l}. \tag{4.3}$$

We also have

$$\cosh\beta_{k,l} + \cosh\delta_{k,l} = -\frac{\kappa_1}{2\kappa_2}, \tag{4.4}$$

from which we obtain

$$2\kappa_2\cosh\beta_{k,l} + \overline{\kappa} = 2\kappa_2(2 - \cosh\delta_{k,l}), \quad 2\kappa_2\cosh\delta_{k,l} + \overline{\kappa} = 2\kappa_2(2 - \cosh\beta_{k,l}). \tag{4.5}$$

The roots also satisfies

$$\cos\beta_{k,l}\cosh\delta_{k,l} = -\frac{\kappa_1}{2\kappa_2}(1 + \lambda_k + \lambda_l) - 1. \tag{4.6}$$

The above relations will be frequently used later on.

Next, we shall exploit the interfacial equations to determine the coefficients $a_{k,l}, b_{k,l}$ and $c_{k,l}$, as in [16] and [3].

We firstly write the interfacial equation at $x_2 = (K-1)\varepsilon$ as

$$(6\kappa_1 + 3\kappa_2/2)\, u_{\rm at}(x) - \kappa_1 \sum_{|x'-x|=\varepsilon} u_{\rm at}(x') - \frac{\kappa_2}{2} u_{\rm cb}(x_1, x_2+2\varepsilon, x_3) - \kappa_2 u_{\rm at}(x_1, x_2-2\varepsilon, x_3) = -\kappa_2\varepsilon.$$

Using the homogeneous equation satisfied by $u_{\rm at}$, we obtain

$$-\frac{\kappa_2}{2}(u_{\rm at}(x_1, (K-1)\varepsilon, x_3) + u_{\rm cb}(x_1, (K+1)\varepsilon, x_3)) + \kappa_2 u_{\rm at}(x_1, (K+1)\varepsilon, x_3) = -\kappa_2\varepsilon. \tag{4.7}$$

Next, we write the interfacial equation at $x_2 = K\varepsilon$ as

$$(6\kappa_1 + 5\kappa_2)\, u_{\rm at}(x) - \kappa_1 \sum_{|x'-x|=\varepsilon, x_2' \neq (K+1)\varepsilon} u_{\rm at}(x') \\ - \overline{\kappa} u_{\rm cb}(x_1, (K+1)\varepsilon, x_3) - \kappa_2 u_{\rm at}(x_1, (K-2)\varepsilon, x_3) = 2\kappa_2\varepsilon.$$

Using the homogeneous equation satisfied by $u_{\rm at}$, we obtain

$$3\kappa_2 u_{\rm at}(x_1, K\varepsilon, x_3) + \kappa_1 u_{\rm at}(x_1, (K+1)\varepsilon, x_3) + \kappa_2 u_{\rm at}(x_1, (K+2)\varepsilon, x_3) \\ - \overline{\kappa} u_{\rm cb}(x_1, (K+1)\varepsilon, x_3) = 2\kappa_2\varepsilon. \tag{4.8}$$

Finally, we write the equation for $x_2 = (K+1)\varepsilon$ as

$$(6\kappa_1 + 17\kappa_2/2)\, u_{\rm cb}(x) - \kappa_1 \sum_{|x'-x|=\varepsilon, x_2' \neq (K+2)\varepsilon, x_2' \neq K\varepsilon} u_{\rm cb}(x') \\ - \overline{\kappa}(u_{\rm cb}(x_1, (K+2)\varepsilon, x_3) + u_{\rm at}(x_1, K\varepsilon, x_3)) - \frac{\kappa_2}{2} u_{\rm at}(x_1, (K-1)\varepsilon, x_3) = -\kappa_2\varepsilon.$$

Using the homogeneous equation satisfied by $u_{\rm cb}$, we obtain

$$\frac{\kappa_2}{2}(u_{\rm cb}(x_1, (K+1)\varepsilon, x_3) - u_{\rm at}(x_1, (K-1)\varepsilon, x_3)) + \overline{\kappa}(u_{\rm cb}(x_1, K\varepsilon, x_3) - u_{\rm at}(x_1, K\varepsilon, x_3)) = -\kappa_2\varepsilon. \tag{4.9}$$

Subtracting (4.7) from (4.9), we obtain

$$\overline{\kappa} u_{\rm cb}(x_1, K\varepsilon, x_3) + \kappa_2 u_{\rm cb}(x_1, (K+1)\varepsilon, x_3) = \overline{\kappa} u_{\rm at}(x_1, K\varepsilon, x_3) + \kappa_2 u_{\rm at}(x_1, (K+1)\varepsilon, x_3).$$

Substituting the expression of u into the above identity, we get

$$a_{k,l} = \frac{g(\beta_{k,l})}{h(\alpha_{k,l})} b_{k,l} + \frac{g(\delta_{k,l})}{h(\alpha_{k,l})} c_{k,l},$$

where g and h are defined by

$$g(x) := \overline{\kappa} \sinh[Kx] + \kappa_2 \sinh[(K+1)x], \\ h(x) := \overline{\kappa} \sinh[(N-K)x] + \kappa_2 \sinh[(N-K-1)x].$$

Denote $\rho_{k,l} := \kappa_2 \sinh[(N-K-1)\alpha_{k,l}]/h(\alpha_{k,l})$. Substituting the expression of $u_{\rm at}$ and $u_{\rm cb}$ into (4.8) and using the discrete Fourier transform, we obtain

$$\phi(\beta_{k,l}) b_{k,l} + \phi(\delta_{k,l}) c_{k,l} = \frac{8\kappa_2\varepsilon}{N^2} \frac{1-(-1)^k}{2} \frac{1-(-1)^l}{2} \cot\frac{k\pi}{2N} \cot\frac{l\pi}{2N},$$

where

$$\phi(x) = 3\kappa_2 \sinh[Kx] + \kappa_1 \sinh[(K+1)x] + \kappa_2 \sinh[(K+2)x] - \frac{\overline{\kappa}}{\kappa_2} \rho_{k,l} g(x).$$

Substituting the expressions of $u_{\rm at}$ and $u_{\rm cb}$ into (4.7) and using the discrete Fourier transform, we obtain

$$\psi(\beta_{k,l}) b_{k,l} + \psi(\delta_{k,l}) c_{k,l} = -\frac{8\kappa_2\varepsilon}{N^2} \frac{1-(-1)^k}{2} \frac{1-(-1)^l}{2} \cot\frac{k\pi}{2N} \cot\frac{l\pi}{2N},$$

where

$$\psi(x) = -\kappa_2 \sinh[(K-1)x] + 2\kappa_2 \sinh[(K+1)x] - \rho_{k,l} g(x).$$

Solving this linear system, we obtain

$$b_{k,l} = \frac{(\phi+\psi)(\delta_{k,l})}{\Delta} \frac{8\kappa_2\varepsilon}{N^2} \frac{1-(-1)^k}{2} \frac{1-(-1)^l}{2} \cot\frac{k\pi}{2N} \cot\frac{l\pi}{2N},$$

and

$$c_{k,l} = -\frac{(\phi+\psi)(\beta_{k,l})}{\Delta} \frac{8\kappa_2\varepsilon}{N^2} \frac{1-(-1)^k}{2} \frac{1-(-1)^l}{2} \cot\frac{k\pi}{2N} \cot\frac{l\pi}{2N},$$

where

$$\Delta = \phi(\beta_{k,l})\psi(\delta_{k,l}) - \phi(\delta_{k,l})\psi(\beta_{k,l}).$$

A direct calculation gives

$$\begin{aligned}\Delta = {} & A_{k,l}\sinh[K\beta_{k,l}]\sinh[K\delta_{k,l}] + B_{k,l}\sinh[K\beta_{k,l}]\cosh[K\delta_{k,l}] \\ & + C_{k,l}\sinh[K\delta_{k,l}]\cosh[K\beta_{k,l}] + D_{k,l}\cosh[K\beta_{k,l}]\cosh[K\delta_{k,l}],\end{aligned} \tag{4.10}$$

where

$$\begin{aligned}&A_{k,l} = \rho_{k,l}\overline{\kappa}[(\tau_{k,l}-1)\overline{\kappa} + \tau_{k,l}(\lambda_k+\lambda_l)\kappa_1](\cosh\delta_{k,l} - \cosh\beta_{k,l}),\\ &B_{k,l} = \rho_{k,l}\sinh\delta_{k,l}\kappa_2^2 F(\beta_{k,l}, \overline{\kappa}/|\kappa_2|), \quad C_{k,l} = -\rho_{k,l}\sinh\beta_{k,l}\kappa_2^2 F(\delta_{k,l}, \overline{\kappa}/|\kappa_2|),\\ &D_{k,l} = -2(3-\rho_{k,l})\kappa_2^2\sinh\beta_{k,l}\sinh\delta_{k,l}(\cosh\delta_{k,l} - \cosh\beta_{k,l}).\end{aligned}$$

Here, for $b = \beta_{k,l}, \delta_{k,l}$,

$$\begin{aligned}F(b,t) := {} & (4\tau_{k,l}(1+\lambda_k+\lambda_l) - \tau_{k,l}\cosh b - 3)t^2 \\ & - 2((\tau_{k,l}-1)(2\cosh b - 1) + (\lambda_k+\lambda_l)(1-8\tau_{k,l}))t - 8(\lambda_k+\lambda_l).\end{aligned}$$

The derivation of the above representation of Δ will be given in Appendix A.

5 Pointwise estimate of the error

5.1 Preliminaries

It follows from Theorem 4.1 that the stability condition $\overline{\kappa}^2 + 8\kappa_1\kappa_2(\lambda_k+\lambda_l) > 0$ for all k, l. By $\kappa_2 < 0$, we immediately have $\overline{\kappa}^2 \geqslant 32\kappa_1|\kappa_2|$. Solving this equation, we obtain

$$\overline{\kappa} > 8(2+\sqrt{6})|\kappa_2|. \tag{5.1}$$

In what follows, we impose a stronger stability condition unless otherwise stated,

$$\overline{\kappa} \geqslant 56|\kappa_2|. \tag{5.2}$$

The following lemma gives a tight bound for $\tau_{k,l}$.

Lemma 5.1. *There holds*

$$\exp\alpha_{k,l} < \tau_{k,l} < \exp\alpha_{k,l} + \exp[-(2N-2K-3)\alpha_{k,l}]. \tag{5.3}$$

Proof. By definition,

$$\tau_{k,l} - \exp\alpha_{k,l} = \frac{\sinh\alpha_{k,l}}{\sinh[(N-K-1)\alpha_{k,l}]}\exp[-(N-k-1)\alpha_{k,l}],$$

which gives the left-hand side of (5.3).

On the other hand, using the elementary inequality

$$\frac{\sinh[(N-K-1)t]}{\sinh t} \geqslant \exp[(N-K-2)t], \quad t \geqslant 0,$$

which implies the right-hand side of (5.3). □

A direct consequence of (5.3) is

$$\tau_{k,l} > \cosh\alpha_{k,l} + \sinh\alpha_{k,l} = 1 + \frac{\kappa_1}{\overline{\kappa}}(\lambda_k+\lambda_l) + \frac{\kappa_1}{\overline{\kappa}}\sqrt{(2\overline{\kappa}/\kappa_1 + \lambda_k+\lambda_l)(\lambda_k+\lambda_l)}, \tag{5.4}$$

which immediately implies

$$\tau_{k,l} \geqslant 1 + \frac{2\kappa_1}{\overline{\kappa}}(\lambda_k+\lambda_l) \geqslant 1 + 2(\lambda_k+\lambda_l), \tag{5.5}$$

and

$$\tau_{k,l} \geqslant 1 + \sqrt{2(\lambda_k+\lambda_l)}. \tag{5.6}$$

The next lemma gives the bounds for $\beta_{k,l}$ and $\delta_{k,l}$.

Lemma 5.2. *There holds*

$$1+\frac{\kappa_1}{\overline{\kappa}}(\lambda_k+\lambda_l)\leqslant\cosh\beta_{k,l}\leqslant 1+\frac{2\kappa_1}{\overline{\kappa}}(\lambda_k+\lambda_l),\tag{5.7}$$

and

$$1+\frac{\overline{\kappa}}{2|\kappa_2|}-\frac{2\kappa_1}{\overline{\kappa}}(\lambda_k+\lambda_l)\leqslant\cosh\delta_{k,l}\leqslant 1+\frac{\overline{\kappa}}{2|\kappa_2|}-\frac{\kappa_1}{\overline{\kappa}}(\lambda_k+\lambda_l).\tag{5.8}$$

Proof. An elementary calculation gives

$$\begin{aligned}\cosh\beta_{k,l}&=1+\frac{\overline{\kappa}}{4|\kappa_2|}(1-\sqrt{1-8\kappa_1|\kappa_2|(\lambda_k+\lambda_l)/\overline{\kappa}^2})\\&=1+\frac{2\kappa_1(\lambda_k+\lambda_l)/\overline{\kappa}}{1+\sqrt{1-8\kappa_1|\kappa_2|(\lambda_k+\lambda_l)/\overline{\kappa}^2}},\end{aligned}$$

which immediately implies (5.7).

Proceeding along the same line, we obtain (5.8). □

Using (5.7), we obtain

$$\sinh[\beta_{k,l}/2]\leqslant 3\bigg(\sin\frac{k\pi}{2N}+\sin\frac{l\pi}{2N}\bigg).\tag{5.9}$$

It is clear that $A_{k,l},D_{k,l}<0$. It follows from (5.7) and (5.8) that

$$\cosh\delta_{k,l}-\cosh\beta_{k,l}\geqslant\frac{\overline{\kappa}}{2|\kappa_2|}-\frac{4\kappa_1}{\overline{\kappa}}(\lambda_k+\lambda_l),$$

which together with (5.2) yields

$$\frac{4\kappa_1}{\overline{\kappa}}(\lambda_k+\lambda_l)\leqslant 16\kappa_1/\overline{\kappa}\leqslant 18\leqslant\frac{1}{3}\frac{\overline{\kappa}}{|\kappa_2|}.$$

This implies

$$\cosh\delta_{k,l}-\cosh\beta_{k,l}\geqslant\frac{\overline{\kappa}}{6|\kappa_2|}.$$

Using (4.4) and (4.6), we obtain

$$\begin{aligned}\sinh^2\beta_{k,l}\sinh^2\delta_{k,l}&=(\cosh\beta_{k,l}\cosh\delta_{k,l}+1)^2-(\cosh\beta_{k,l}+\cosh\delta_{k,l})^2\\&=\frac{\kappa_1^2}{4\kappa_2^2}(\lambda_k+\lambda_l)(2+\lambda_k+\lambda_l).\end{aligned}$$

Combining the above two inequalities, we bound

$$|D_{k,l}|\geqslant\sqrt{(\lambda_k+\lambda_l)/2}\,\overline{\kappa}^2.\tag{5.10}$$

It remains to determine the signs of $B_{k,l}$ and $C_{k,l}$, which depend on the following two lemmas.

Lemma 5.3. *Let $\Lambda=8(2+\sqrt{6})$. If the stability condition* (5.1) *holds true, then for all k,l and $t\geqslant\Lambda$, we have*

$$F(\beta_{k,l},t)>0.\tag{5.11}$$

Lemma 5.4. *Let $\Lambda_1=56$. If the stability condition* (5.2) *holds true, then for all k,l and $t\geqslant\Lambda_1$, we have*

$$F(\delta_{k,l},t)<0.$$

By Lemma 5.3, we conclude that $B_{k,l}=\rho_{k,l}\sinh\delta_{k,l}\kappa_2^2F(\beta_{k,l},\overline{\kappa}/|\kappa_2|)<0$. By Lemma 5.4, we conclude that $C_{k,l}=|\rho_{k,l}|\sinh\beta_{k,l}\kappa_2^2F(\delta_{k,l},\overline{\kappa}/|\kappa_2|)<0$. The proof for the above two lemmas are postponed to Appendix B.

We are ready to bound $|\Delta|$ from below.

Lemma 5.5. *Under* (5.2)*, there holds*

$$|\Delta| \geqslant \frac{\sqrt{2}}{8}\overline{\kappa}^2\sqrt{\lambda_k+\lambda_l}\exp[K(\beta_{k,l}+\delta_{k,l})]. \tag{5.12}$$

Proof. Because $A_{k,l}, B_{k,l}, C_{k,l}$ and $D_{k,l}$ are negative for all k, l, we obtain

$$|\Delta| \geqslant |D_{k,l}|\cosh[K\beta_{k,l}]\cosh[K\delta_{k,l}],$$

which together with (5.10) yields (5.12). □

Remark 5.6. We are not intending to pursue a tight lower bound for Δ, while the order is optimal because it is easy to find that $|A_{k,l}|, |B_{k,l}|, |C_{k,l}| = \mathcal{O}(\sqrt{\lambda_k+\lambda_l}\,\overline{\kappa}^2)$.

5.2 Pointwise estimate of the error

We firstly write $\rho_{k,l}$ as

$$\rho_{k,l} = \frac{\kappa_2}{\tau_{k,l}\overline{\kappa}+\kappa_2} \quad \text{with} \quad \tau_{k,l} := \frac{\sinh[(N-k)\alpha_{k,l}]}{\sinh[(N-K-1)\alpha_{k,l}]},$$

and $1-(\overline{\kappa}/\kappa_2+1)\rho_{k,l} = (\tau_{k,l}-1)\rho_{k,l}\overline{\kappa}/\kappa_2$. Using (A.1) and (A.2) in Appendix A and the above identity, we obtain

$$|(\phi+\psi)(x)| \leqslant C\overline{\kappa}\sqrt{\lambda_k+\mu_l}\exp[Kx], \quad x = \beta_{k,l}, \delta_{k,l}. \tag{5.13}$$

The following lemma is similar to [3, Lemma 5.2], the proof is slightly different.

Lemma 5.7. *For* $1 \leqslant k, l \leqslant N$*, we have*

$$\exp[-\beta_{k,l}] \leqslant \exp\left[-\frac{k+l}{2N}\right], \quad \exp[-\alpha_{k,l}] \leqslant \exp\left[-\frac{k+l}{2N}\right], \tag{5.14}$$

$$\exp[-\delta_{k,l}] \leqslant \frac{3|\kappa_2|}{2\overline{\kappa}}. \tag{5.15}$$

Proof. Using (5.7), we have

$$\begin{aligned}\exp[\beta_{k,l}] &\geqslant 1+\sinh\beta_{k,l} \geqslant 1+\sqrt{2(\lambda_k+\lambda_l)}\\ &\geqslant 1+\sqrt{2}\left(\sin\frac{k\pi}{2N}+\sin\frac{l\pi}{2N}\right)\\ &\geqslant 1+\frac{\sqrt{2}(k+l)}{N}.\end{aligned}$$

Using the elementary inequality,

$$\ln(1+x) \geqslant \frac{2x}{2+x}, \quad x>0,$$

we obtain

$$\ln(1+\sqrt{2}(k+l)/N) \geqslant \frac{2(k+l)}{\sqrt{2}N+k+l} \geqslant \frac{k+l}{2N}.$$

Combining the above two inequalities, we obtain

$$\exp[-\beta_{k,l}] \leqslant (1+\sqrt{2}(k+l)/N)^{-1} = \exp[-\ln(1+\sqrt{2}(k+l)/N)] \leqslant \exp\left[-\frac{k+l}{2N}\right].$$

This gives the upper bound for $\exp[-\beta_{k,l}]$. The upper bound for $\exp[-\alpha_{k,l}]$ is similar, we omit the details.

Note that

$$\sinh\delta_{k,l} \geqslant \frac{\overline{\kappa}}{3|\kappa_2|}, \tag{5.16}$$

which implies (5.15) by using $\exp[\delta_{k,l}] \geqslant 2\sinh[\delta_{k,l}]$. □

Based on all the previous results, we are ready to bound Du. We only bound D_2u, the estimates for D_1u and D_3u are similar.

A direct calculation gives, for $q \leqslant K-1$,

$$\begin{aligned} D_2u(p,q,r) = \frac{\kappa_2}{N^2} \sum_{\substack{k,l=1\\ k,l \text{ odd}}}^{N} \frac{1}{\Delta}((\phi+\psi)(\delta_{k,l})\cosh[(q+1/2)\beta_{k,l}]\sinh[\beta_{k,l}/2] \\ - (\phi+\psi)(\beta_{k,l})\cosh[(q+1/2)\delta_{k,l}]\sinh[\delta_{k,l}/2]) \\ \times \sin\frac{pk\pi}{N}\cot\frac{k\pi}{2N}\sin\frac{rl\pi}{N}\cot\frac{l\pi}{2N}, \end{aligned}$$

and for $q \geqslant K+1$,

$$\begin{aligned} D_2u(p,q,r) = \frac{\kappa_2}{N^2} \sum_{\substack{k,l=1\\ k,l \text{ odd}}}^{N} \frac{(\phi+\psi)(\delta_{k,l})g(\beta_{k,l}) - (\phi+\psi)(\beta_{k,l})g(\delta_{k,l})}{\Delta h(\alpha_{k,l})} \cosh\left[\left(N-q-\frac{1}{2}\right)\alpha_{k,l}\right]\sinh\left[\frac{\alpha_{k,l}}{2}\right] \\ \times \sin\frac{pk\pi}{N}\cot\frac{k\pi}{2N}\sin\frac{rl\pi}{N}\cot\frac{l\pi}{2N}. \end{aligned}$$

It follows from the above expression that $D_2u(p,q,r) = D_2u(N-p,q,r) = D_2u(p,q,N-r)$. Therefore, we only consider $1 \leqslant p,r \leqslant N/2$. Using (5.13)–(5.15) and (5.9), we have, for $q \leqslant K-1$, there holds

$$\begin{aligned} |D_2u(p,q,r)| &\leqslant C\frac{|\kappa_2|}{\overline{\kappa}N^2} \sum_{\substack{k,l=1\\ k,l \text{ odd}}}^{N} \left(\exp[-|K-q-1/2|\beta_{k,l}]\left(\sin\frac{k\pi}{2N}+\sin\frac{l\pi}{2N}\right)\right. \\ &\quad \left. + \exp[-|K-q|\delta_{k,l}]\right)\cot\frac{k\pi}{2N}\cot\frac{l\pi}{2N} \\ &\leqslant C\frac{|\kappa_2|}{\overline{\kappa}N^2} \sum_{\substack{k,l=1\\ k,l \text{ odd}}}^{N} \exp[-(K-q-1/2)(k+l)/(2N)]\cos\frac{k\pi}{2N}\cot\frac{l\pi}{2N} \\ &\quad + C\frac{|\kappa_2|}{\overline{\kappa}N^2}\left(|\kappa_2|/\overline{\kappa}\right)^{K-q-1/2} \sum_{\substack{k,l=1\\ k,l \text{ odd}}}^{N} \cot\frac{k\pi}{2N}\cot\frac{l\pi}{2N}. \end{aligned}$$

Denoting $\varrho = \exp[-(K-q-1/2)/(2N)]$, we rewrite the above inequality as

$$|D_2u(p,q,r)| \leqslant C\frac{|\kappa_2|}{\overline{\kappa}N^2} \sum_{\substack{l=1\\ l \text{ odd}}}^{N} \varrho^l \cot\frac{l\pi}{2N} \sum_{\substack{k=1\\ k \text{ odd}}}^{N} \varrho^k + C\frac{|\kappa_2|}{\overline{\kappa}N^2}(|\kappa_2|/\overline{\kappa})^{K-q-1/2}\left(\sum_{\substack{l=1\\ l \text{ odd}}}^{N} \cot\frac{l\pi}{2N}\right)^2.$$

Using Lozarević's inequality [9] $\cosh t \leqslant (\frac{\sinh t}{t})^3, t \neq 0$, and the elementary inequality $\cosh t \geqslant \mathrm{e}^t/2, t \in \mathbb{R}$, we obtain

$$\sum_{\substack{k=1\\ k \text{ odd}}}^{N} \varrho^k \leqslant \frac{\varrho}{1-\varrho^2} = \frac{1}{2\sinh[(K-q)/(2N)]} \leqslant \frac{2N}{K-q}\exp\left[-\frac{(K-q)}{6N}\right].$$

Using the inequality $\cot x \leqslant 1/x$ for $x > 0$, we obtain

$$\sum_{\substack{l=1\\ l \text{ odd}}}^{N} \varrho^l \cot\frac{l\pi}{2N} \leqslant \frac{2N}{\pi}\sum_{\substack{l=1\\ l \text{ odd}}}^{N}\frac{\varrho^l}{l} \leqslant \frac{2N}{\pi}\sum_{\substack{l=1\\ l \text{ odd}}}^{\infty}\frac{\varrho^l}{l} = \frac{N}{\pi}\ln\frac{1+\varrho}{1-\varrho} \leqslant CN\ln\frac{N}{K-q-1/2}.$$

Proceeding along the same line that leads to the above inequality, we obtain

$$\sum_{\substack{l=1\\ k,l \text{ odd}}}^{N} \cot\frac{l\pi}{2N} \leqslant \frac{2N}{\pi}\sum_{\substack{l=1\\ k,l \text{ odd}}}^{N}\frac{1}{l} \leqslant CN\ln N.$$

To sum up, we obtain

$$|D_2u(p,q,r)|\leqslant C\frac{|\kappa_2|}{\overline{\kappa}}\frac{\ln\left(N/(K-q-1/2)\right)}{K-q-1/2}+C\left(\frac{|\kappa_2|}{\overline{\kappa}}\right)^{K-q+1/2}\ln^2 N.$$

We deal with $q=K,K+1$ separately. If $q=K$, then we have

$$|D_1u(p,q,r)|\leqslant C\frac{|\kappa_2|}{\overline{\kappa}N}\sum_{\substack{l=1\\ l\text{ odd}}}^{N}\cot\frac{l\pi}{2N}+C\frac{|\kappa_2|^2}{\overline{\kappa}^2N}\sum_{\substack{l=1\\ l\text{ odd}}}^{N}\cot\frac{l\pi}{2N}\leqslant C\frac{|\kappa_2|}{\overline{\kappa}}\ln N.$$

When $q\geqslant K+1$, notice the following identity:

$$\begin{aligned}&(\phi+\psi)(\delta_{k,l})g(\beta_{k,l})-(\phi+\psi)(\beta_{k,l})g(\delta_{k,l})\\&\quad=\kappa_1(\lambda_k+\lambda_l)(\sinh[K\delta_{k,l}]g(\beta_{k,l})-\sinh[K\beta_{k,l}]g(\delta_{k,l}))\\&\qquad+2\kappa_2(1-\cosh\beta_{k,l})\sinh\delta_{k,l}\cosh[K\delta_{k,l}]g(\beta_{k,l})\\&\qquad+2\kappa_2(\cosh\delta_{k,l}-1)\sinh\beta_{k,l}\cosh[K\beta_{k,l}]g(\delta_{k,l}),\end{aligned}$$

and using (5.13), we have

$$|D_2u(p,q,r)|\leqslant C\frac{|\kappa_2|}{\overline{\kappa}N^2}\sum_{\substack{k=1\\ l\text{ odd}}}^{N}\varrho^k\cos\frac{k\pi}{2N}\sum_{\substack{l=1\\ l\text{ odd}}}^{N}\varrho^l\cot\frac{l\pi}{2N}\leqslant C\frac{|\kappa_2|}{\overline{\kappa}}\frac{\ln N/(q+1/2-K)}{q+1/2-K}.$$

Summing up the above estimate, we have the following theorem.

Theorem 5.8. *There exists C such that*

$$|Du(p,q,r)|\leqslant C\frac{|\kappa_2|}{\overline{\kappa}}\frac{\ln N/|K-q-1/2|}{|K-q-1/2|}+C\left(\frac{|\kappa_2|}{\overline{\kappa}}\right)^{K-q+1/2}\ln^2 N,\tag{5.17}$$

where C is independent of ε.

Remark 5.9. If $p=1$ or $r=1$, then the above estimate can be improved to

$$|Du(p,q,r)|\leqslant C\frac{|\kappa_2|}{\overline{\kappa}}\frac{\ln N/|K-q-1/2|}{|K-q-1/2|^2}+C\left(\frac{|\kappa_2|}{\overline{\kappa}}\right)^{K-q+1/2}\ln N.$$

If $p=r=1$, then we have the improved estimate as

$$|Du(1,q,1)|\leqslant C\frac{|\kappa_2|}{\overline{\kappa}}|K-q-1/2|^{-3}+C\left(\frac{|\kappa_2|}{\overline{\kappa}}\right)^{K-q+1/2}.$$

The estimate (5.17) is far from optimal in two aspects compared to the numerical results. First, it is hard to judge whether the presence of the logarithmic factor in (5.17) is due to the tricks we employed or it is essential, while it seems that $\|Du\|_\infty$ increases slightly when N is small as suggested by Table 7. Second, the decay rate should be one half as suggested by Table 2. We believe the estimate (5.17) can be improved by refining the argument, which however seems quite subtle and we shall pursue it in other publication. Instead, we give a heuristic explanation about this conjecture by using the lattice Green's function.

Let the interface Γ be the $x-y$ plane, and $f(x)$ takes the same form as that in (3.1) with x_2 replaced by x_3. Denote by $m(x)=\mathrm{dist}(x,\Gamma)/\varepsilon$, then

$$|Du(x)|\leqslant\frac{C}{1+m^2(x)},\tag{5.18}$$

where C is independent of ε.

By the definition of the Green's function associated with $\mathcal{L}_{\rm qc}$, we have $u(x)=\sum_y G(x;y)f(y)$, where y runs over the support of f. Notice that the source term f is a discrete delta function supported in the vicinity of the interface, we write

$$u(x)=\varepsilon^2\sum_{y_2,y_3}(G(x;-\varepsilon,y_2,y_3)-2G(x;0,y_2,y_3)+G(x;\varepsilon,y_2,y_3))=\varepsilon^4\sum_{y_2,y_3}D_{y_1}^2G(x;0,y_2,y_3),\quad(5.19)$$

which implies

$$D_xu(x)=\varepsilon^4\sum_{y_2,y_3}D_xD_{y_1}^2G(x;0,y_2,y_3).$$

If the following estimate for the Green's function is true,

$$|D_xD_y^2G(x;y)|\leqslant\frac{C}{|x-y|^4+\varepsilon^4},\quad(5.20)$$

where C is independent of ε, then we have

$$\begin{aligned}|D_xu(x)|&\leqslant\varepsilon^4\sum_{y_2,y_3}|D_xD_y^2G(x;0,y_2,y_3)|\\&=C\sum_{y_2,y_3}\frac{1}{1+|x_1/\varepsilon|^4+|(x_2-y_2)/\varepsilon|^4+|(x_3-y_3)/\varepsilon|^4}\\&=C\sum_{n',p'}\frac{1}{1+m^4(x)+(n-n')^4+(p-p')^4}.\end{aligned}$$

The above sum can be estimated as follows. We give the details for estimating one item of the above sum for brevity.

$$\begin{aligned}\sum_{n'=1}^{n-1}\sum_{p'=1}^{p-1}\frac{1}{1+m^4(x)+(n-n')^4+(p-p')^4}&\leqslant\sum_{n'=1}^{n-1}\sum_{p'=1}^{p-1}\frac{8}{(1+m(x))^4+8n'^4+8p'^4}\\&\leqslant8\sum_{n'=1}^{n-1}\int_0^{p'-1}\frac{1}{(1+m(x))^4+8n'^4+8s^4}\mathrm{d}\,s\\&\leqslant64\sum_{n'=1}^{n-1}\int_0^{p'-1}\frac{1}{(1+m(x)+n')^4+64s^4}\mathrm{d}\,s\\&\leqslant C\sum_{n'=1}^{n-1}(1+m(x)+n')^{-3}\leqslant\frac{C}{1+m^2(x)}.\end{aligned}$$

This gives (5.18).

The above procedure is quite general, while it heavily depends on the following two facts: (1) the special structure of f that makes the error into a discrete gradient as (5.19); (2) the pointwise estimate for the lattice Greens function (5.20), which may not be available for $\mathcal{L}_{\rm qc}$, while such estimate is true for $\mathcal{L}_{\rm cb}$ and we refer to [8] for related results.

6 Conclusion

Based on a series of models with different complexity, we have shown that

(1) the ghost force leads to a finite size error over the displacement gradient, while the magnitude of such an error is quite small, which is usually related to the ratio among the elastic constants;

(2) the error has a layer-like profile, and the width of the interfacial layer is of $\mathcal{O}(\varepsilon)$;

(3) the error in the displacement gradient decays algebraically from $\mathcal{O}(1)$ to $\mathcal{O}(\varepsilon)$ away from the interface.

The first point is not new, while it actually justifies the linearized model or even the harmonic lattice model. The second point seems new, while it is actually hidden in the previous study for one-dimensional and two-dimensional problems. Our study together with the previous investigation suggest that the $\mathcal{O}(\varepsilon)$-layer width is generic for problems in one, two and three dimensions. The last point is new while the sharp decay rate is still unknown.

It is worth mentioning that the surrogate model tells the same story for the effect of the ghost force, while it is much simpler and analytically tractable. Whether such surrogate model can be trusted deserves further tests for more realistic cases. We note that a similar surrogate model has been exploited to study the effect of the ghost force for the dynamic problems in one dimension [11].

The present approach does not seem to apply to the nonplanar a/c interface. A possible way to do this is the approach presented in the end of Sections, which relies on the structure of the ghost force and the estimate of the lattice Green's function associated with the method.

Acknowledgments

This work was supported by National Natural Science Foundation of China (Grant Nos. 10932011, 91230203 and 11021101) and Chinese Academy of Science National Center for Mathematics and Interdisciplinary Sciences. The authors thank Professor Weinan E for inspiring discussions on the topic studied here.

References

1 Abraham F F, Broughton J Q, Bernstein N, et al. Spanning the coninuum to quantum length scales in a dynamic simulation of brittle fracture. Europhys Lett, 1998, 44: 783–787
2 Born M, Huang K. Dynamical Theory of Crystal Lattices. Oxford: Oxford University Press, 1954
3 Chen J R, Ming P B. Ghost force influence of a quasicontinuum method in two dimension. J Comput Math, 2012, 30: 657–683
4 Dobson M, Luskin M. An analysis of the effect of ghost force oscillation on quasicontinuum error. Math Model Numer Anal, 2009, 43: 591–604
5 E W. Principles of Multiscale Modeling. Cambridge: Cambridge University Press, 2011
6 E W, Lu J, Yang J Z. Uniform accuracy of the quasicontinuum method. Phys Rev B, 2006, 74: 214115
7 Knap J, Ortiz M. An analysis of the quasicontinuum method. J Mech Phys Solids, 2011, 49: 1899–1923
8 Lawler G F. Intersections of Random Walks. Boston, MA: Birkhäuser, 1991
9 Lazarević I. Neke nejednakosti sa hiperbolickim funkcijama. Univerzitet u Beogradu, Publikacije Elektrotehničkog Fakulteta, Serija Matematika i Fizika, 1966, 170: 41–48
10 Lennard-Jones J E. On the determination of molecular fields, II: From the equation of state of a gas. Proc Roy Soc London Ser A, 1924, 106: 463–477
11 Li X T, Ming P B. On the effect of ghost force in the quasicontinuum method: Dynamic problems in one dimension. ArXiv:1208.1321
12 Lu J, Ming P B. Stability of a force-based hybrid method in three dimension with sharp interface. ArXiv:1212.3643v1
13 Lu J, Ming P B. Convergence of a force-based hybrid method in three dimensions. Comm Pure Appl Math, 2013, 66: 83–108
14 Miller R E, Tadmor E B. A unified framework and performance benchmark of fourteen multiscale atomistic/continuum coupling methods. Modelling Simul Mater Sci Eng, 2009, 17: 053001–053051
15 Ming P B. Error estimate of force-based quasicontinuum method. Commun Math Sci, 2008, 6: 1087–1095
16 Ming P B, Yang J Z. Analysis of a one-dimensional nonlocal quasi-continuum method. Multiscale Model Simul, 2009, 7: 1838–1875
17 Ortner C. The role of the patch test in 2D atomistic-to-continuum coupling methods. Math Model Numer Anal, 2012, 46: 1275–1319
18 Shapeev A V. Consistent energy-based atomistic/continuum coupling for two-body potentials in three dimensions. SIAM J Sci Comput, 2012, 34: 335–360
19 Shenoy V B, Miller R, Tadmor E B, et al. An adaptive finite element approach to atomic scale mechanics—the quasicontinuum method. J Mech Phys Solids, 1999, 47: 611–642
20 Tadmor E B, Ortiz M, Phillips R. Quasicontinuum analysis of defects in solids. Philos Mag A, 1996, 73: 1529–1536

A Explicit form for Δ

We firstly write $\phi(x)$ as

$$\phi(x) = (3\kappa_2 + \kappa_1 \cosh x + \kappa_2 \cosh[2x]) \sinh[Kx] + (\kappa_1 \sinh x + \kappa_2 \sinh[2x]) \cosh[Kx] - (\overline{\kappa}/\kappa_2)\rho_{k,l} g(x).$$

Using (4.3), we get, for $x = \beta_{k,l}, \delta_{k,l}$,

$$\begin{aligned} 3\kappa_2 + \kappa_1 \cosh x + \kappa_2 \cosh[2x] &= 2\kappa_2 + \kappa_1 \cosh x + 2\kappa_2 \cosh^2 x = \kappa_1(1 + \lambda_k + \lambda_l) + 4\kappa_2 \\ &= \overline{\kappa} + \kappa_1(\lambda_k + \lambda_l). \end{aligned}$$

It follows from (4.4) that

$$\begin{aligned} \kappa_1 \sinh x + \kappa_2 \sinh[2x] &= (\kappa_1 + 2\kappa_2 \cosh x) \sinh x \\ &= \begin{cases} -2\kappa_2 \cosh \delta_{k,l} \sinh \beta_{k,l}, & x = \beta_{k,l}, \\ -2\kappa_2 \cosh \beta_{k,l} \sinh \delta_{k,l}, & x = \delta_{k,l}. \end{cases} \end{aligned}$$

Using the above two identities, we obtain

$$\begin{aligned} \phi(\beta_{k,l}) &= (\overline{\kappa} + \kappa_1(\lambda_k + \lambda_l)) \sinh[K\beta_{k,l}] - 2\kappa_2 \cosh \delta_{k,l} \sinh \beta_{k,l} \cosh[K\beta_{k,l}] - (\overline{\kappa}/\kappa_2)\rho_{k,l} g(\beta_{k,l}), \\ \phi(\delta_{k,l}) &= (\overline{\kappa} + \kappa_1(\lambda_k + \lambda_l)) \sinh[K\delta_{k,l}] - 2\kappa_2 \cosh \beta_{k,l} \sinh \delta_{k,l} \cosh[K\delta_{k,l}] - (\overline{\kappa}/\kappa_2)\rho_{k,l} g(\delta_{k,l}). \end{aligned}$$

Similarly,

$$\psi(x) = \kappa_2 \cosh x \sinh[Kx] + 3\kappa_2 \sinh x \cosh[Kx] - \rho_{k,l} g(x),$$

where

$$x = \beta_{k,l}, \delta_{k,l}.$$

A direct calculation gives

$$\begin{aligned} (\phi + \psi)(\beta_{k,l}) &= (\overline{\kappa} + \kappa_1(\lambda_k + \lambda_l) + \kappa_2 \cosh \beta_{k,l}) \sinh[K\beta_{k,l}] \\ &\quad + \kappa_2 \sinh \beta_{k,l} \cosh[K\beta_{k,l}] + 2\kappa_2(1 - \cosh \delta_{k,l}) \sinh \beta_{k,l} \cosh[K\beta_{k,l}] \\ &\quad - (\overline{\kappa}/\kappa_2 + 1)\rho_{k,l} g(\beta_{k,l}) \\ &= \kappa_1(\lambda_k + \lambda_l) \sinh[K\beta_{k,l}] + 2\kappa_2(1 - \cosh \delta_{k,l}) \sinh \beta_{k,l} \cosh[K\beta_{k,l}] \\ &\quad + (1 - (\overline{\kappa}/\kappa_2 + 1)\rho_{k,l}) g(\beta_{k,l}), \end{aligned} \tag{A.1}$$

and

$$\begin{aligned} (\phi + \psi)(\delta_{k,l}) &= \kappa_1(\lambda_k + \lambda_l) \sinh[K\delta_{k,l}] + 2\kappa_2(1 - \cosh \beta_{k,l}) \sinh \delta_{k,l} \cosh[K\delta_{k,l}] \\ &\quad + (1 - (\overline{\kappa}/\kappa_2 + 1)\rho_{k,l}) g(\delta_{k,l}). \end{aligned} \tag{A.2}$$

To calculate Δ, we expand $\phi(x) + \psi(x)$ and $\psi(x)$ for $x = \beta_{k,l}$ as

$$\begin{aligned} (\phi + \psi)(\beta_{k,l}) &= \left(\kappa_1(\lambda_k + \lambda_l) + (\tau_{k,l} - 1)\rho_{k,l} \frac{\overline{\kappa}}{\kappa_2}(\overline{\kappa} + \kappa_2 \cosh \beta_{k,l})\right) \sinh[K\beta_{k,l}] \\ &\quad + (2\kappa_2(1 - \cosh \delta_{k,l}) + (\tau_{k,l} - 1)\rho_{k,l}\overline{\kappa}) \sinh \beta_{k,l} \cosh[K\beta_{k,l}], \end{aligned} \tag{A.3}$$

and

$$\psi(\beta_{k,l}) = (\kappa_2 \cosh \beta_{k,l}(1 - \rho_{k,l}) - \rho_{k,l}\overline{\kappa}) \sinh[K\beta_{k,l}] + (3 - \rho_{k,l})\kappa_2 \sinh \beta_{k,l} \cosh[K\beta_{k,l}],$$

using

$$(1 - \rho_{k,l})\kappa_2 = \tau_{k,l}\rho_{k,l}\overline{\kappa},$$

we write

$$\psi(\beta_{k,l}) = (\tau_{k,l} \cosh \beta_{k,l} - 1)\rho_{k,l}\overline{\kappa} \sinh[K\beta_{k,l}] + (3 - \rho_{k,l})\kappa_2 \sinh \beta_{k,l} \cosh[K\beta_{k,l}].$$

Similar equations hold true for $(\phi + \psi)(\delta_{k,l})$ and $\psi(\delta_{k,l})$. Substituting the above equations into

$$\Delta = \phi(\beta_{k,l})\psi(\delta_{k,l}) - \phi(\delta_{k,l})\psi(\beta_{k,l}) = (\phi + \psi)(\beta_{k,l})\psi(\delta_{k,l}) - (\phi + \psi)(\delta_{k,l})\psi(\beta_{k,l}),$$

we obtain (4.10).

B Proofs of Lemmas 5.3 and 5.4

Proof of Lemma 5.3. Using (5.7), we obtain

$$\begin{aligned}4\tau_{k,l}(1+\lambda_k+\lambda_l)-\tau_{k,l}\cosh\beta_{k,l}-3&=\tau_{k,l}(1+4\lambda_k+4\lambda_l-\cosh\beta_{k,l})+3(\tau_{k,l}-1)\\&\geqslant(4-2\kappa_1/\overline{\kappa})\,(\lambda_k+\lambda_l)\tau_{k,l}+3(\tau_{k,l}-1)\\&\geqslant(\lambda_k+\lambda_l)\tau_{k,l}+3(\tau_{k,l}-1),\end{aligned}$$

which together with

$$F(\beta_{k,l},0)=-8(\lambda_k+\lambda_l)<0$$

implies $F(\beta_{k,l},t)\geqslant F(\beta_{k,l},\Lambda)$ for $t\geqslant\Lambda$. A direct calculation gives

$$\begin{aligned}F(\beta_{k,l},\Lambda)\geqslant{}&(\Lambda^2-8)(\lambda_k+\lambda_l)+(\tau_{k,l}-1)(3\Lambda-2\cosh\beta_{k,l})\Lambda\\&+2\,(\tau_{k,l}-1-\lambda_k-\lambda_l)\,\Lambda+16\Lambda\tau_{k,l}(\lambda_k+\lambda_l).\end{aligned}$$

Using (5.7), we have

$$3\Lambda-2\cosh\beta_{k,l}\geqslant3\Lambda-2+\lambda_k+\lambda_l.$$

Under the stability condition (5.1), we conclude that

$$\begin{aligned}F(\beta_{k,l},\Lambda)&\geqslant(3\Lambda^2+2\Lambda-2)(\tau_{k,l}-1)+(\Lambda^2+14\Lambda-8)(\lambda_k+\lambda_l)+17\Lambda(\tau_{k,l}-1)(\lambda_k+\lambda_l)\\&>3\Lambda^2(\tau_{k,l}-1)>0.\end{aligned}$$

This gives (5.11) and completes the proof. □

Proof of Lemma 5.4. Using (5.8) and the stability condition (5.2), we get

$$\begin{aligned}4\tau_{k,l}(1+\lambda_k+\lambda_l)-\tau_{k,l}\cosh\delta_{k,l}-3&=\tau_{k,l}(4+4\lambda_k+4\lambda_l-\cosh\delta_{k,l})-3\\&\leqslant\tau_{k,l}\bigg(3-\frac{\overline{\kappa}}{2|\kappa_2|}+(6+8|\kappa_2|/\overline{\kappa})(\lambda_k+\lambda_l)\bigg)-3\\&\leqslant-3.\end{aligned}$$

Invoking the stability condition (5.2) again, we obtain

$$\begin{aligned}&(\tau_{k,l}-1)(2\cosh\delta_{k,l}-1)+(\lambda_k+\lambda_l)(1-8\tau_{k,l})\\&\quad\geqslant(\tau_{k,l}-1)\,(1+\overline{\kappa}/|\kappa_2|-(12+16(|\kappa_2|/\overline{\kappa}))\,(\lambda_k+\lambda_l))-7(\lambda_k+\lambda_l)\\&\quad\geqslant5(\tau_{k,l}-1)-7(\lambda_k+\lambda_l)\geqslant3(\lambda_k+\lambda_l)>0,\end{aligned}$$

where we have used (5.5) in the next-to-last step.

The above two inequalities together with the fact $F(\delta_{k,l},0)<0$ leads to

$$F(\delta_{k,l},t)\leqslant F(\delta_{k,l},\Lambda_1)\quad\text{for}\quad t\geqslant\Lambda_1.$$

A direct calculation gives

$$\begin{aligned}F(\delta_{k,l},\Lambda_1)&\leqslant-3\Lambda_1^2-8(\lambda_k+\lambda_l)-2((\tau_{k,l}-1)(2\cosh\delta_{k,l}-1)+(\lambda_k+\lambda_l)(1-8\tau_{k,l}))\Lambda_1\\&=-2(\tau_{k,l}-1)(2\cosh\delta_{k,l}-1-8\lambda_k-8\lambda_l)\Lambda_1-8(\lambda_k+\lambda_l)+(14(\lambda_k+\lambda_l)-3\Lambda_1)\Lambda_1\\&\leqslant-2(\tau_{k,l}-1)(58-4(\kappa_1/\overline{\kappa}+2)(\lambda_k+\lambda_l))\Lambda_1-2\Lambda_1^2.\end{aligned}$$

Using the stability condition (5.2), we get $58-4(\kappa_1/\overline{\kappa}+2)(\lambda_k+\lambda_l)>0$. A combination of the above three inequalities completes the proof. □